# Emergence of Simple Patterns in Complex Atomic Nuclei from First Principles

**T. Dytrych**[1,2]**, K. D. Launey**[1]**, J. P. Draayer**[1]**, P. Maris**[3]**, J. P. Vary**[3]**, D. Langr**[4,5]**, T. Oberhuber**[6]

[1] Department of Physics and Astronomy, Louisiana State University, Baton Rouge, LA 70803, USA
[2] Nuclear Physics Institute, 250 68 Řež, Czech Republic
[3] Department of Physics and Astronomy, Iowa State University, Ames, IA 50011, USA
[4] Faculty of Information Technology, Czech Technical University, Prague 16000, Czech Republic
[5] Aerospace Research and Test Establishment, Prague 19905, Czech Republic
[6] Faculty of Nuclear Sciences and Physical Engineering, Czech Technical University, Prague 11519, Czech Republic

E-mail: `tdytrych@phys.lsu.edu`

**Abstract.** We study the structure of low-lying states in $^6$Li, $^6$He, $^8$Be, $^8$B, $^{12}$C, and $^{16}$O, using *ab initio* symmetry-adapted no-core shell model. The results of our study demonstrate that collective modes in light nuclei emerge from first principles. We investigate the impact of the symmetry-adapted model space on spectroscopic properties and, in the case of the ground state of $^6$Li, on elastic electron scattering charge form factor. The results confirm that only a small symmetry-adapted subspace of the complete model space is needed to accurately reproduce complete-space observables and the form factor momentum dependence.

## 1. Introduction

*Ab initio* approaches to nuclear structure and reactions have advanced our understanding and capability of achieving first-principle descriptions of light nuclei [1, 2, 3]. These advances are driven by the major progress in the development of realistic nuclear potential models, such as J-matrix inverse scattering potentials [4] and two- and three-nucleon potentials derived from meson exchange theory [5] or by using chiral effective field theory [6], and, at the same time, by the utilization of massively parallel computing resources [7, 8, 9]. The *ab initio* applications to heavier systems has been hindered by computational challenges. While the Coupled Cluster [10] and selfconsistent Greens function methods [11] can be applied to probe medium-mass nuclei in the vicinity of shell closures, for nuclei far from closures, innovative approaches has just started to emerge [12]. These new developments place serious demands on available computational resources. This points to the need of further major advances in many-body methods to access a wider range of nuclei and experimental observables, while retaining the predictive power of *ab initio* methods, which makes them suitable for e.g. targeting short-lived nuclei that are inaccessible by experiment but essential to further modeling, for example, of the dynamics of X-ray bursts and the path of nucleosynthesis (see, e.g., [13, 14]).

The main challenge of *ab initio* configuration-interaction approaches is inherently coupled

with the combinatorial growth in the size of the many-particle model space with the increasing number of nucleons and expansion in the number of single-particle levels in the model space. This rapid growth motivates us to develop and investigate a novel model, the *ab initio* symmetry-adapted no-core shell model (SA-NCSM) [15].

The SA-NCSM adopts the first-principle concept and joins a no-core shell model (NCSM) with an SU(3)-based coupling scheme [16]. The NCSM [2] calculations are carried out in many-particle basis constructed from harmonic oscillator (HO) single-particle states characterized by the HO frequency $\hbar\Omega$. The model space is spanned by nuclear configurations of fixed parity, consistent with the Pauli principle, and truncated by a cutoff $N_{\max}$. The $N_{\max}$ cutoff is defined as the maximum number of HO quanta allowed in a many-particle state above the minimum for a given nucleus.

The many-nucleon basis states of the SA-NCSM for a given $N_{\max}$ are constructed in SU(3)-coupled proton-neutron formalism and are labeled as

$$|\vec{\gamma}; N(\lambda\,\mu)\kappa L; (S_p S_n S); JM\rangle, \tag{1}$$

where the quantum numbers $S_p$, $S_n$, and $S$ denote proton, neutron, and total intrinsic spins, respectively. The label $N$ signifies the number of HO quanta with respect to the minimal number for a given nucleus, and $(\lambda\,\mu)$ represent a set of quantum numbers associated with SU(3) irreducible representations, irreps. The label $\kappa$ distinguishes multiple occurrences of the same orbital momentum $L$ in the parent irrep $(\lambda\,\mu)$. The $L$ is coupled with $S$ to the total angular momentum $J$ and its projection $M$. The symbol $\vec{\gamma}$ schematically denotes the additional quantum numbers needed to unambiguously distinguish between irreps carrying the same $N(\lambda\,\mu)(S_p S_n S)$ quantum numbers.

In the current implementation of SA-NCSM, $\vec{\gamma}$ specifies a distribution of nucleon clusters over the major HO shells and their inter-shell coupling. Specifically, in each major HO shell $\eta$ with degeneracy $\Omega_\eta$, nucleon clusters are arranged into antisymmetric $U(\Omega_\eta) \times SU(2)_{S_\eta}$ irreps [17], with $U(\Omega_\eta)$ further reduced with respect to SU(3). The quantum numbers, $\left[f_1, \ldots, f_{\Omega_\eta}\right] \alpha_\eta(\lambda_\eta\,\mu_\eta)S_\eta$, along with $SU(3)\times SU(2)_S$ labels of inter-shell coupling unambigiously determine SA-NCSM basis states (1). Note that a spatial symmetry associated with a Young shape $\left[f_1, \ldots, f_{\Omega_\eta}\right]$ is uniquely determined by the imposed antisymmetrization and the associated intrinsic spin $S_\eta$. A multiplicity index $\alpha_\eta$ is required to distinguish multiple ocurrences of SU(3) irrep $(\lambda_\eta\,\mu_\eta)$ in a given $U(\Omega_\eta)$ irrep. The SA-NCSM basis states (1) bring forward important information about nuclear shapes and deformation according to an established mapping [18]. For example, $(00)$, $(\lambda\,0)$ and $(0\,\mu)$ describe spherical, prolate and oblate shapes, respectively.

## 2. Emergence of Collective Modes in Light Nuclei

The significance of the SU(3) group for a microscopic description of the nuclear collective dynamics can be seen from the fact that it is the symmetry group of the successful Elliott model [16], and a subgroup of the physically relevant $Sp(3,\mathbb{R})$ symplectic model [19], which provides a comprehensive theoretical foundation for understanding the dominant symmetries of nuclear collective motion.

To explore the nature of the most important many-nucleon correlations, we analyze the four lowest-lying isospin-zero ($T = 0$) states of $^6$Li ($1^+_{\text{gs}}$, $3^+_1$, $2^+_1$, and $1^+_2$), the ground-state rotational bands of $^8$Be, $^6$He and $^{12}$C, the lowest $1^+$, $3^+$, and $0^+$ excited states of $^8$B, and the ground state of $^{16}$O. We study the probability distribution across Pauli-allowed $(S_p S_n S)$ and $(\lambda\,\mu)$ configurations.

Results for the ground state of $^6$Li and $^8$Be, obtained with the JISP16 and chiral N$^3$LO interactions, respectively, are shown in Figures 1 and 2. These figures illustrate a feature
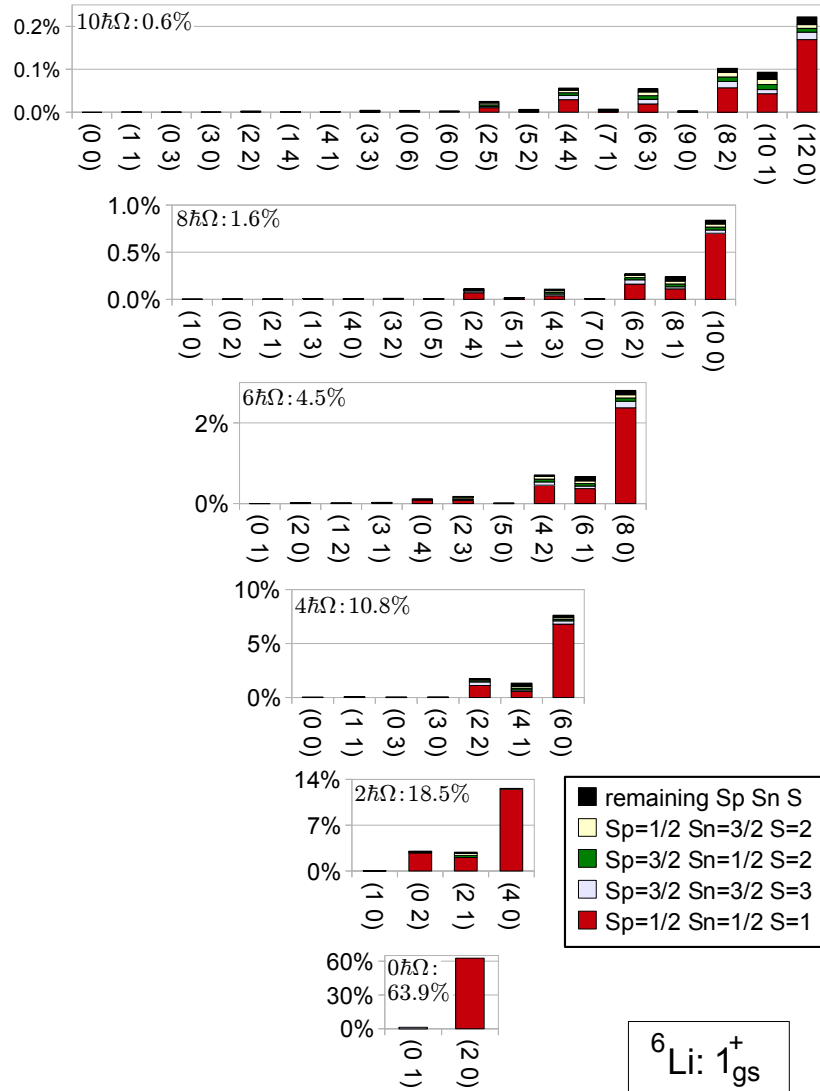
**Figure 1.** Probability distributions for proton, neutron, and total intrinsic spin components $(S_p S_n S)$ across the Pauli-allowed $(\lambda \mu)$ values (horizontal axis) for the calculated $1^+$ ground state of $^6$Li obtained for $N_{\max} = 10$ and $\hbar\Omega = 20$ MeV with the JISP16 interaction. The total probability for each $N\hbar\Omega$ subspace is given in the upper left-hand corner of each histogram.

common to all the low-energy solutions considered. In particular, a highly structured and regular mix of intrinsic spins and SU(3) spatial quantum numbers, which, furthermore, does not seem to depend on the particular choice of realistic $NN$ potential.

For a closer look at these results, first consider the spin content. We found that the calculated eigenstates project at a 99% level onto a comparatively small subset of intrinsic spin combinations. These combinations are characterized by the lowest allowed values of proton and neutron spins, $S_p$ and $S_n$, and favor the total intrinsic spin $S$ with maximal value, i.e. $S = S_p + S_n$. For instance, the ground state bands in even-even nuclei, e.g. $^8$Be, $^6$He, $^{12}$C, and $^{16}$O, are found to be dominated by many-particle configurations carrying total intrinsic
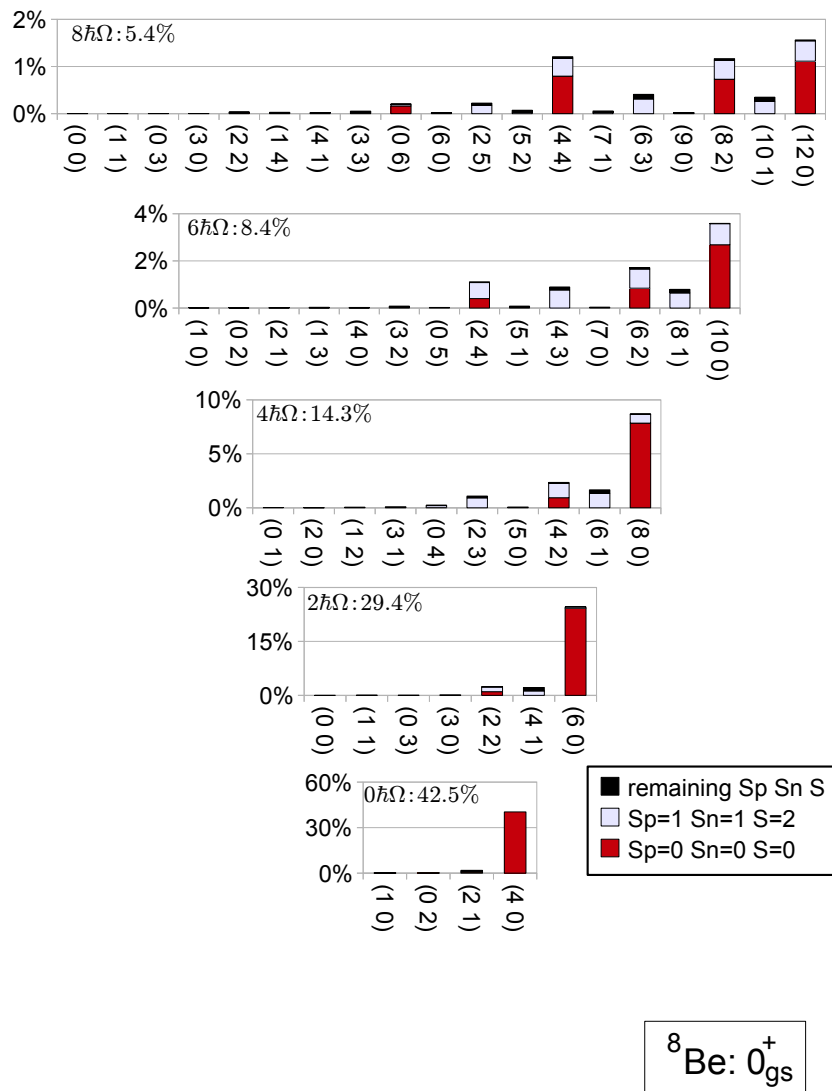
**Figure 2.** Probability distributions for proton, neutron, and total intrinsic spin components $(S_p S_n S)$ across the Pauli-allowed $(\lambda \mu)$ values (horizontal axis) for the calculated $0^+$ ground state of $^8$Be obtained for $N_{\max} = 8$ and $\hbar\Omega = 25$ MeV with the chiral N$^3$LO interaction. The total probability for each $N\hbar\Omega$ subspace is given in the upper left-hand corner of each histogram. The concentration of strengths to the far right within the histograms demonstrates the dominance of collectivity in the calculated eigenstates.

| Nucleus | $(S_p\, S_n\, S)$ | Prob. [%] | $(\lambda_0\, \mu_0)$ | Prob. [%] |
|---------|-------------------|-----------|-----------------------|-----------|
| $^6$Li  | $(\frac{1}{2}\,\frac{1}{2}\,1)$ | 93.26 | $(2\,0)$ | 98.13 |
| $^8$B   | $(\frac{1}{2}\,\frac{1}{2}\,1)$ | 85.17 | $(2\,1)$ | 87.94 |
| $^8$Be  | $(0\,0\,0)$ | 85.25 | $(4\,0)$ | 90.03 |
| $^{12}$C | $(0\,0\,0)$ | 55.19 | $(0\,4)$ | 48.44 |
| $^{16}$O | $(0\,0\,0)$ | 83.60 | $(0\,0)$ | 89.51 |

**Table 1.** Total probabilities of the dominant $(S_p\, S_n\, S)$ spin configuration and the dominant nuclear shapes according to Eq. (2) for the ground state of $p$-shell nuclei.

spin of the protons and neutrons equal to zero and one, with the largest contributions due to $(S_pS_nS)$=(000) and (112) configurations. The lowest-lying eigenstates in $^6$Li are almost entirely realized in terms of configurations characterized by the following intrinsic spin $(S_pS_nS)$ combinations: $(\frac{1}{2}\frac{1}{2}1)$, $(\frac{3}{2}\frac{3}{2}3)$, $(\frac{1}{2}\frac{3}{2}2)$, and $(\frac{3}{2}\frac{1}{2}2)$, where the first combination is carrying over 90% of each eigenstate. Likewise, the same spin components as in the case of $^6$Li are found to dominate the ground state and the lowest $1^+$, $3^+$, and $0^+$ excited states of $^8$B (Table 1).

Second, consider the spatial degrees of freedom. Our results show that the mixing of $(\lambda\, \mu)$ quantum numbers, induced by the SU(3) symmetry breaking terms of realistic interactions, exhibits a remarkably simple pattern. One of its key features is the preponderance of a single $0\hbar\Omega$ SU(3) irrep. This so-called leading irrep, according to the established geometrical interpretation of SU(3) labels $(\lambda\, \mu)$ [18], is characterized by the largest value of the intrinsic quadrupole deformation. For instance, the low-lying states of $^6$Li project at a 40%-70% level onto the prolate $0\hbar\Omega$ SU(3) irrep $(2\,0)$, as illustrated in Figs. 1 and 2 for the ground state. For the considered states of $^8$B, $^8$Be, $^{12}$C, and $^{16}$O, qualitatively similar dominance of the leading $0\hbar\Omega$ SU(3) irreps is observed – $(2\,1)$, $(4\,0)$, $(0\,4)$, and $(0\,0)$ irreps, associated with triaxial, prolate, oblate, and spherical shapes, respectively. The clear dominance of the most deformed $0\hbar\Omega$ configuration within low-lying states of light $p$-shell nuclei indicates that the quadrupole-quadrupole interaction of the Elliott SU(3) model of nuclear rotations [16] is realized naturally within an *ab initio* framework.

The analysis also reveals that the dominant SU(3) basis states at each $N\hbar\Omega$ subspace $(N = 0, 2, 4, \dots)$ are typically those with $(\lambda\, \mu)$ quantum numbers given by

$$\lambda + 2\mu = \lambda_0 + 2\mu_0 + N \qquad (2)$$

where $\lambda_0$ and $\mu_0$ denote labels of the leading SU(3) irrep in the $0\hbar\Omega$ ($N = 0$) subspace. Furthermore, there is an apparent hierarchy among states that fulfill condition (2). In particular, the $N\hbar\Omega$ configurations with $(\lambda_0+N\ \mu_0)$, the so-called stretched states, carry a noticeably higher probability than the others. For instance, the $(2+N\ 0)$ stretched states contribute at the 85% level to the ground state of $^6$Li, as can be readily seen in Fig. 1. Moreover, the dominance of the stretched states is rapidly increasing with the increasing many-nucleon basis cutoff $N_{\max}$.

## 3. Efficacy of Symmetry-Adapted Concept
The observed simple patterns of intrinsic spin and deformation mixing supports a symmetry-adapted selection of configuration space that takes advantage of dominant symmetries and refines the definition of the NCSM model space, which is based solely on the $N_{\max}$ cutoff.

To accommodate highly-deformed configurations (high-energy HO excitations) together with essential mixing of low-energy excitations, typical SA-NCSM calculations span the complete space up to a given $N_{\max}^{\perp}$, while beyond this, calculations include only selected many-nucleon basis states limited by the $N_{\max}$ cutoff. At each $N\hbar\Omega$ space, where $N^{\perp} < N \leq N_{\max}$, we select many-nucleon basis states carrying a fixed set of $(S_p S_n S)$ and $(\lambda\, \mu)$ quantum numbers. It is
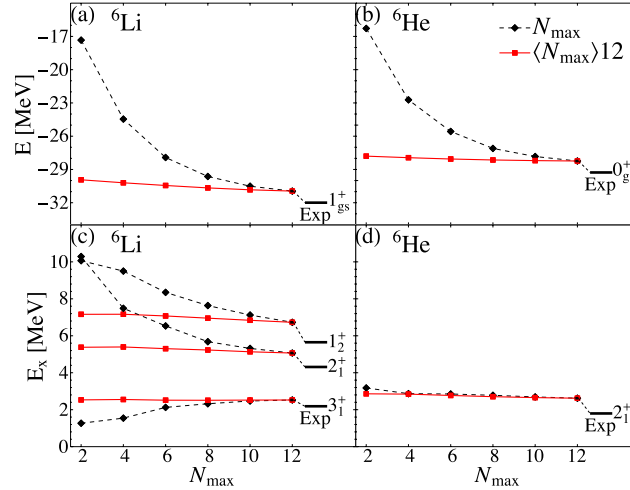
**Figure 3.** The ground-state binding energies of $^6$Li (a) and $^6$He (b), excitation energies of $T = 0$ states of $^6$Li (c), $2^+_1$ excited state of $^6$He (d), shown for the complete $N_{max}$ (dashed black curves) and truncated $\langle N^\perp_{max} = N_{max}\rangle 12$ (solid red lines) model spaces. Results shown are for JISP16 and $\hbar\Omega = 20$ MeV. Note the relatively large changes when the complete space is increased from $N_{max} = 2$ to $N_{max} = 12$ as compared to nearly constant $\langle N_{max}\rangle 12$ SA-NCSM outcomes.

important to note that such a defined model space keeps ability to factorize the center-of-mass motion exactly [20]. As a result, an SA-NCSM model space defined by a set of dominant U(3) irreps $N(\lambda\,\mu)$ and important intrinsic spins, $(S_p S_n S)$, yields eigensolutions with the center-of-mass in the HO ground state. We adopt a notation where, for example, an SA-NCSM model space of "$\langle 4\rangle 12$" includes all the configurations up through $N^\perp_{max} = 4$ and a restricted subspace beyond $N^\perp_{max} = 4$ up through $N_{max} = 12$. When we quote only the $N_{max}$ value, it is understood that the space is complete through that $N_{max}$ (for example $N_{max} = 8 = N^\perp_{max}$).

The efficacy of the symmetry-adapted concept is illustrated for SA-NCSM results obtained in model spaces which are expanded beyond a complete $N^\perp_{max}$ space with irreps that span a relatively few dominant intrinsic spin components and carry quadrupole deformation specified by Eq. (2). Specifically, we vary $N^\perp_{max}$ from 2 to 10 with only the subspaces determined by Eq. (2) included beyond $N^\perp_{max}$. This allows us to study convergence of spectroscopic properties towards results obtained in the complete $N_{max} = 12$ space and hence, probes the efficacy of the symmetry-adapted model space selection concept. We use a Coulomb plus JISP16 $NN$ interaction for $\hbar\Omega$ values ranging from 17.5 up to 25 MeV, along with the Gloeckner-Lawson prescription [21] for elimination of spurious center-of-mass excitations. SA-NCSM eigenstates are used to determine spectroscopic properties of low-lying $T = 0$ states of $^6$Li and the ground-state band of $^6$He for $\langle N^\perp_{max}\rangle 12$ model spaces.

The results indicate that the observables obtained in the $\langle N^\perp_{max}\rangle 12$ symmetry-adapted truncated spaces are excellent approximations to the corresponding $N_{max} = 12$ complete-space
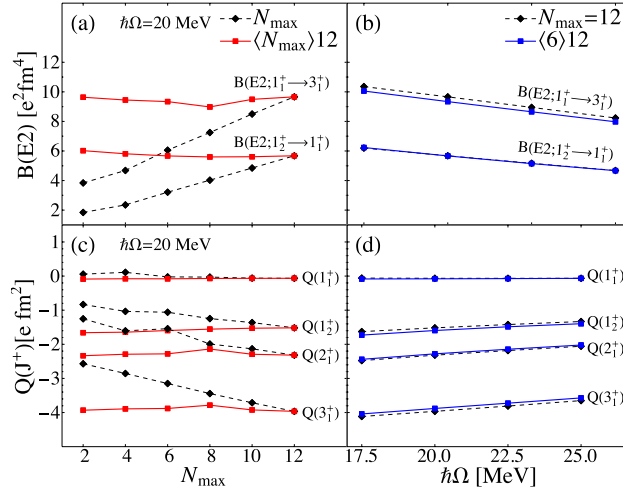
**Figure 4.** Electric quadrupole transition probabilities and quadrupole moments for $T = 0$ states of $^6$Li calculated using the JISP16 interaction without using effective charges are shown for the complete $N_{max}$ (dashed black lines) and truncated $\langle N^\perp_{max} = N_{max}\rangle 12$ (solid red lines) model spaces [(a) and (c)], and as a function of $\hbar\Omega$ for the complete $N_{max} = 12$ space and $\langle 6\rangle 12$ truncated space (solid blue lines) [(b) and (d)]. Experimentally, $B(E2; 1^+_1 \rightarrow 3^+_1) = 25.6(20)\, e^2\text{fm}^4$ [24].

counterparts. Furthermore, the level of agreement achieved is only marginally dependent on $N^\perp_{max}$. In particular, the ground-state binding energies obtained in a $\langle 2\rangle 12$ model space represent approximately 97% of the complete-space $N_{max} = 12$ binding energy in the case of $^6$Li and reach over 98% for $^6$He [Fig. 3 (a) and (b)]. The excitation energies differ only by 5 keV to a few hundred keV from the corresponding complete-space $N_{max} = 12$ results [see Fig. 3 (c) and (d)].

The electric quadrupole moments and the reduced electromagnetic $B(E2)$ transition strengths are reproduced remarkably well by the SA-NCSM for $^6$He in the restricted $\langle 8\rangle 12$ space. Notably, the $\langle 2\rangle 12$ eigensolutions for $^6$Li yield results for $B(E2)$ strengths and quadrupole moments that track closely with their complete $N_{max} = 12$ space counterparts (see Fig. 4). It is known that further expansion of the model space beyond $N_{max} = 12$ is needed to reach convergence [22, 23]. However, the close correlation between the $N_{max} = 12$ and $\langle 2\rangle 12$ results is strongly suggestive that this convergence can be obtained through the leading SU(3) irreps in a symmetry-adapted space.

*3.1. Electron-scattering Form Factors*
We also study the impact of the symmetry-adapted model space selection on the elastic electron scattering charge form factors for the ground state of $^6$Li for momentum transfer up to $q \approx 4$ fm$^{-1}$. Namely, we examine the longitudinal form factor ($C0$) for a range of $\hbar\Omega = 15, 20$, and 25 MeV and for several SU(3)-selected spaces, $\langle 2\rangle 12, \langle 4\rangle 12, \langle 6\rangle 12, \langle 8\rangle 12, \langle 10\rangle 12$, together with

the complete $N_{\max} = 12$ space. We use the realistic nucleon-nucleon interactions N2LOopt [25] and JISP16 [4]. The $C0$ form factor is a Fourier transform of the charge density, and hence it provides an indication on how well nuclear wave functions reproduce the low- and higher-momentum components of the nuclear charge density. This, in turn, can reveal important underlying physics responsible for achieving convergence of nuclear radii.

The charge form factors are calculated in the first-order plane-wave Born approximation. They have center-of-mass contribution removed and are further adjusted to account for the finite proton size. They are derived using the formalism and an extension of the computer code developed by Lee [27], described in detail in Ref. [28], as well as using an SU(3)-based apparatus [29, 30] for calculating charge and current density distributions in terms of the shell-model one-body density matrix elements (OBDMEs) and the single-particle matrix elements of the associated electromagnetic operators.

Longitudinal electron scattering form factors for the ground state of $^6$Li are studied for the bare JISP16 and N2LOopt $NN$ interactions up to $N_{\max} = 12$ spaces. An important result is that in all cases, $\langle 6 \rangle 12$ selected-space results are found to be almost identical to the complete-space counterparts in low- and intermediate-momentum regions (Fig. 5), and even above 3 fm$^{-1}$ (not shown in the figure). This remains valid for various $\hbar\Omega$ values, as well as when different interactions are employed (Fig. 5a and b). This further confirms the validity of the symmetry-adapted concept in the SA-NCSM. Indeed, the present results indicate that using these selected spaces, that constitute only a fraction of the complete model space (about 1% for $\langle 6 \rangle 12$), reproduces, in addition, the complete-space form factor momentum dependence. In short, symmetry-adapted model-space selection, which is based on a straightforward prescription dictated by the approximate dynamical symmetries, eliminates many-nucleon basis states that are shown in this study to be also irrelevant for describing the single-proton momentum distribution for the $^6$Li ground state as revealed by the $C0$ form factor at low/intermediate momentum transfers and above.

Deviations in the form factor as a result of the SU(3)-based selection of model spaces are found to decrease for higher $\hbar\Omega$ values (see Fig. 5: the higher the $\hbar\Omega$ value, the narrower the curve). This effect is more prominent for momenta $q > 2$ fm$^{-1}$. The outcome suggests that for high enough $\hbar\Omega$ values, results are almost independent from the model-space truncation and, for $\hbar\Omega = 25$ MeV, the $\langle 2 \rangle 12$ form factor already reproduces the complete-space result. For low $\hbar\Omega$ values, larger $N_{\max}^{\perp}$ spaces ($\langle 4 \rangle 12$ or $\langle 6 \rangle 12$) appear necessary pointing to a mixing of more deformation/spin configurations within these low-$\hbar\Omega$ spaces. However, while low values, $\hbar\Omega < 15$ MeV, are known to require larger model spaces to obtain convergence of the ground state energy, such a mixing at the $4\hbar\Omega$ and $6\hbar\Omega$ subspaces is expected to decrease for $N_{\max} > 12$. In short, the SU(3)-based truncation of the model space yields reasonably small deviations in the form factor, especially for $q < 2$ fm$^{-1}$ and for $\hbar\Omega > 15$ MeV.

While results using N2LOopt lie slightly closer to experiment, both interactions show similar patterns with a small dependence on $\hbar\Omega$(Fig. 5). Furthermore, as one increases $N_{\max}$ (e.g., from $N_{\max} = 8$ to $N_{\max} = 12$), SA-NCSM predictions are reasonably trending towards experiment, as illustrated for a $\langle 6 \rangle N_{\max}$ selected space and for the reasonable $\hbar\Omega = 20$ MeV in Fig. 6. We note that the $N_{\max} = 12$ results continue to deviate from the experimental data for intermediate momenta, especially for $q \gtrsim 2$ fm$^{-1}$. Agreement with experiment could be improved if contributions of three-body interactions in the SA-NCSM calculations and of two-body operators in the $F_L^2$ were included.

## 4. Conclusions
We have developed a novel *ab initio* approach, SA-NCSM, that capitalizes on SU(3) symmetry-adapted physically relevant many-particle basis. We analyzed the structure of low-lying states in $p$-shell nuclei obtained with JISP16, N2LOopt, and chiral N3LO $NN$ realistic interactions
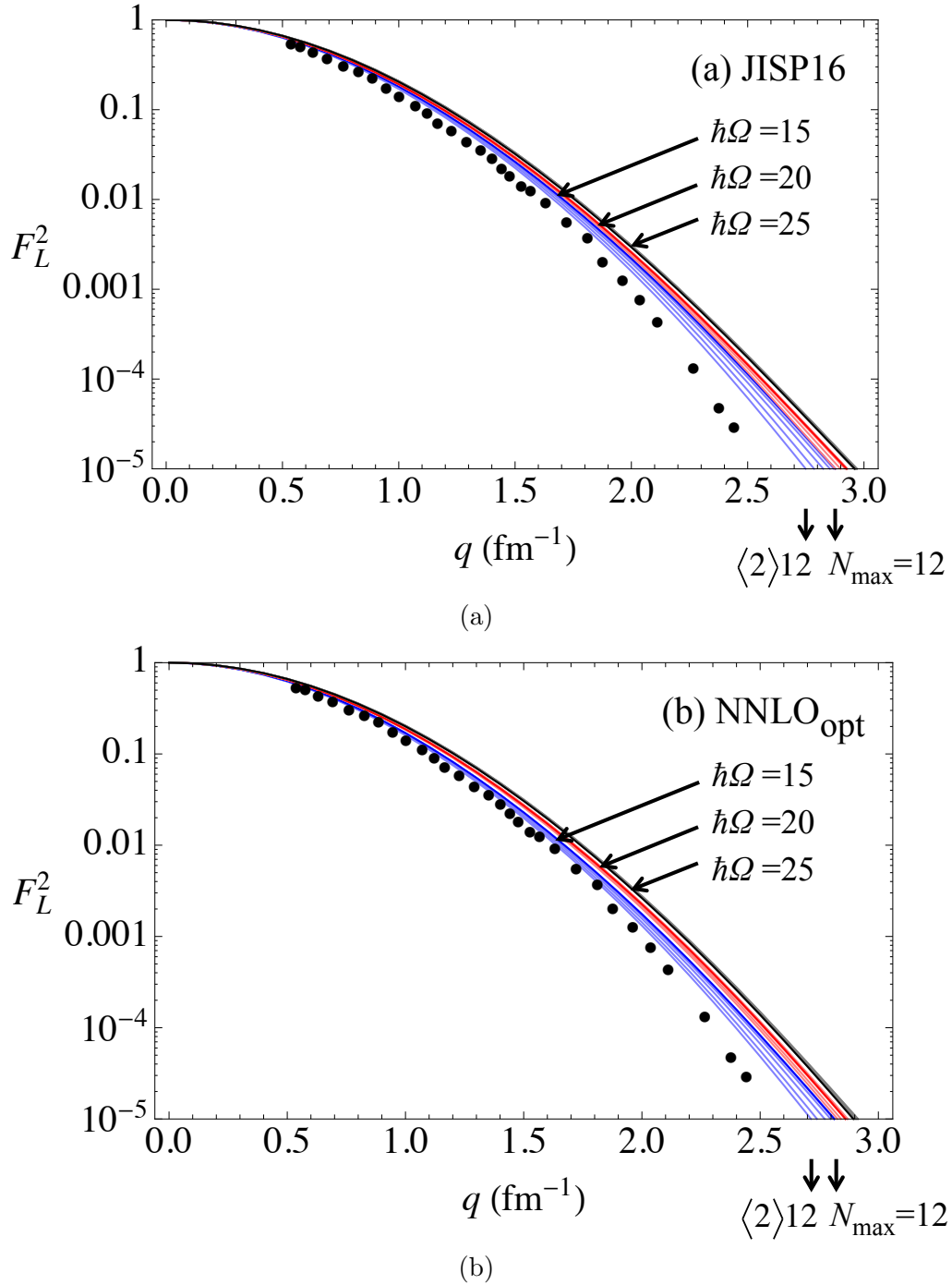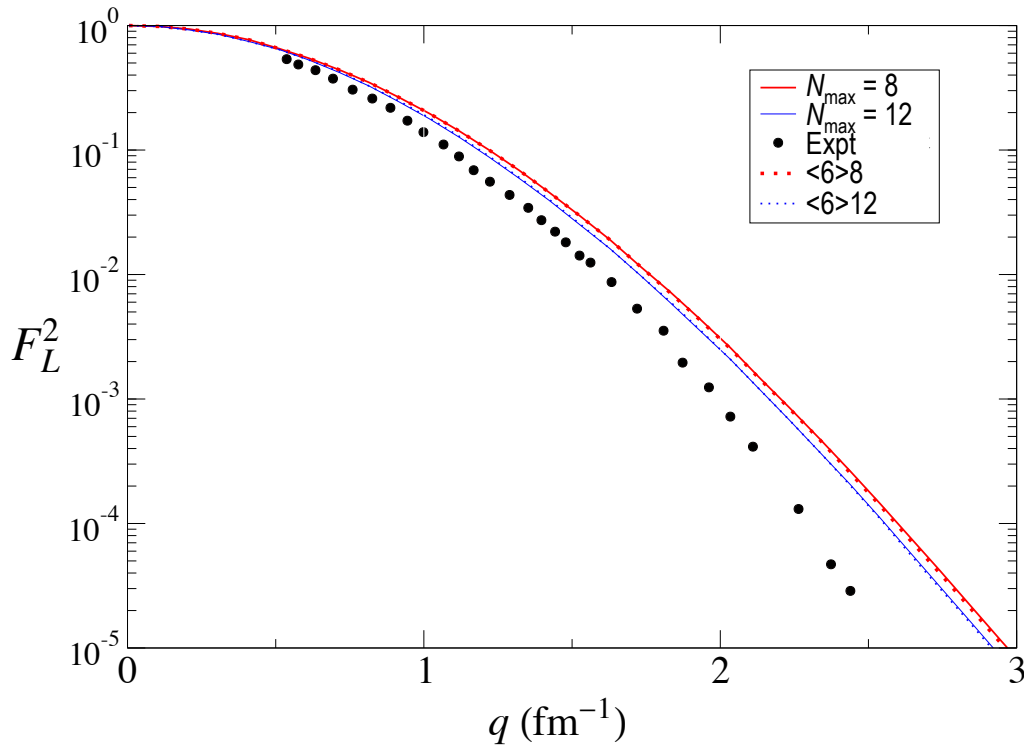
**Figure 5.** Longitudinal $C0$ electron scattering form factors $F_L^2$ (translationally invariant) for the SA-NCSM $1^+$ ground state of $^6$Li calculated in the complete $N_{max} = 12$ space (darker colors) and the SU(3)-selected spaces, $\langle 2 \rangle 12$, $\langle 4 \rangle 12$, $\langle 6 \rangle 12$, $\langle 8 \rangle 12$, and $\langle 10 \rangle 12$ (lighter colors), for $\hbar\Omega = 15$ MeV or $b = 1.66$ fm (blue), $\hbar\Omega = 20$ MeV or $b = 1.44$ fm (red), and $\hbar\Omega = 25$ MeV or $b = 1.29$ fm (black) for (a) the bare JISP16 interaction, as well as for (b) the bare N$^2$LOopt interaction. Experimental data are taken from Ref. [26].

**Figure 6.** Longitudinal $C0$ electron scattering form factors $F_L^2$ (translationally invariant) for the SA-NCSM $1^+$ ground state of $^6$Li calculated for $\hbar\Omega = 20$ MeV or $b = 1.44$ fm and with the bare JISP16 interaction. The outcome for the SU(3)-selected spaces, $\langle 6 \rangle 8$ (red dots) and $\langle 6 \rangle 12$ (blue dots), accurately reproduces the corresponding results for the complete $N_{max} = 8$ space (solid, red) and $N_{max} = 12$ space (solid, blue), with larger-space $N_{max} = 12$ results lying slightly closer to experiment [26].

and complete $N_{max}$ model spaces. The resulting wave functions are dominated by many-nucleon basis states with large quadrupole deformations and low intrinsic spins. This simple orderly pattern does not seem to depend on the particular choice of realistic $NN$ potential. The results demonstrate that observed collective phenomena in light nuclei emerge naturally from first-principles considerations. It is important to note that signatures that hint to the emergence of rotational motion were recently observed also in Be isotopes [31].

We carried out the calculations of the binding energies, excitation energies, electromagnetic moments, E2 and M1 reduced transitions, for selected states in $^6$Li and $^6$He obtained with the symmetry-adapted model spaces. We have shown that the SA-NCSM reduces the configuration space to physically relevant subspaces without compromising the accuracy of *ab initio* NCSM approach. Furthermore, we demonstrated that the symmetry-adapted model space properly treats low- and higher-momentum components of the $^6$Li ground state charge density. The outcome confirms the utility of the SA-NCSM concept for low-lying nuclear states.

### Acknowledgments

## References

[1] Pieper S C Wiringa R B and Carlson J 2004 *Phys. Rev.* C **70** 054325
    Nollett K M Pieper S C Wiringa R B Carlson J and Hale G M 2007 *Phys. Rev. Lett.* **99** 022502
[2] Navrátil P Vary J P and Barrett B R 2000 *Phys. Rev. Lett.* **84** 5728
    Navrátil P Vary J P and Barrett B R 2000 *Phys. Rev.* C **62** 054311
    Quaglioni S and Navrátil P 2008 *Phys. Rev. Lett.* **101** 092501
    Quaglioni S and Navrátil P 2009 *Phys. Rev.* C **79** 044606
    Barrett B R Navrátil P and Vary J P 2013 *Prog. Part. Nucl. Phys.* **69** 131
[3] Hagen G Dean D J Hjorth-Jensen M Papenbrock T and Schwenk A 2007 *Phys. Rev.* C **76** 044305
[4] Shirokov A M Mazur A I Zaytsev S A Vary J P and Weber T A 2004 *Phys. Rev.* **70** 044005
    Shirokov A M Vary J P Mazur A I Zaytsev S A and Weber T A 2005 *Phys. Lett.* B **621** 96
    Shirokov A M Vary J P Mazur A I and Weber T A 2007 *Phys. Lett.* B **644** 33
[5] Machleidt R Sammarruca F and Song Y 1996 *Phys. Rev.* C **53** R1483
    Machleidt R 2001 *Phys. Rev.* C **63** 024001
[6] Entem D R and Machleidt R 2003 *Phys. Rev.* C **68** 041001
[7] Sternberg P Ng E G Yang C Maris P Vary J P Sosonkina M and Le H V 2008 In Proc. 2008 ACM/IEEE Conf. on Supercomputing Austin November 2008 IEEE Press Piscataway NJ 15:1
[8] Maris P Sosonkina M Vary J P Ng E G and Yang C 2010 *Procedia Computer Science* **1** 97
[9] Aktulga H M Yang C Ng E N Maris P and Vary J P 2012 *Lecture Notes on Computer Science* **7484** 830
[10] Hagen G Papenbrock T Dean D J and Hjorth-Jensen M 2008 *Phys. Rev. Lett.* **101** 092502
    Hagen G Papenbrock T and Hjorth-Jensen M 2010 *Phys. Rev. Lett.* **104** 182501
[11] Cipollone A Barbieri C and Navrátil P 2013 *Phys. Rev. Lett.* **111** 062501
[12] Hergert H Binder S Calci A Langhammer J and Roth R 2013 *Phys. Rev. Lett.* **110** 242501
[13] Davids B Cyburt R H Jose J and Mythili S 2011 *Astrophys. J.* **735** 40
[14] Laird A M Parikh A Murphy A S J Wimmer K Chen A A Deibel C M Faestermann T Fox S P Fulton B R Hertenberger R Irvine D José J Longland R Mountford D J Sambrook B Seiler D and Wirth H F 2013 *Phys. Rev. Lett.* **110** 032502
[15] Dytrych T Launey K D Draayer J P Maris P Vary J P Saule E Catalyurek U Sosonkina M Langr D and Caprio M A 2013 *Phys. Rev. Lett.* **111** 252501
[16] Elliott J P 1958 *Proc. Roy. Soc.* A **245** 128
    Elliott J P 1958 *Proc. Roy. Soc.* A **245** 562
    Elliott J P and Harvey M 1962 *Proc. Roy. Soc.* A **272** 557
[17] Draayer J P Leschber Y Park S C and Lopez R 1989 *Comput. Phys. Comm.* **56** 279
[18] Castaños O Draayer J P and Leschber Y 1988 *Z. Phys* **329** 33
    Rosensteel G and Rowe D J 1977 *Ann. Phys. N.Y.* **104** 134
    Leschber Y and Draayer J P 1987 *Phys. Lett.* B **190** 1
[19] Rosensteel G and Rowe D J 1977 *Phys. Rev. Lett.* **38** 10
[20] Verhaar B J 1960 *Nucl. Phys.* A **21** 508
[21] Gloeckner D H and Lawson R D 1974 *Phys. Lett.* B **53** 313
[22] Cockrell C Vary J P and Maris P 2012 *Phys. Rev.* C **86** 034325
[23] Maris P and Vary J P 2013 *Int. J. Mod. Phys.* E **22** 1330016
[24] Tilley D R Cheves C M Godwin J L Hale G M Hofmann H M Kelley J H Sheu C G and Weller H R 2002 *Nucl. Phys.* A **708** 3
[25] Ekström A Baardsen G Forssén C Hagen G Hjorth-Jensen M Jansen G R Machleidt R Nazarewicz W Papenbrock T Sarich J and Wild S M 2013 *Phys. Rev. Lett.* **110** 192502
[26] Li G C Sick I Whitney R R and Yearian M R 1971 *Nucl. Phys.* A **162** 583
[27] Lee H C 1974 *Atomic Energy Canada Limited Report* AECL-4839 (unpublished)
[28] Hayes A C and Kwiatkowski A A 2010 *Phys. Rev.* C **81** 054301
[29] Rochford P and Draayer J P 1992 *Ann. Phys.* **214** 341
[30] Escher J and Draayer J P 1999 *Phys. Rev. Lett.* **82** 5221
[31] Caprio M A Maris P and Vary J P 2013 *Phys. Lett.* B **719** 179
    Maris P Caprio M A and Vary J P 2015 *Phys. Rev.* C **91** 014310